Supporting Information for

Reticular Assembly of 1D and 2D Cu_{10} Cluster-Assembled Materials as Recyclable Luminescent Probe for Highly Sensitive Creatinine Detection

Tsukasa Irie,[†] *Riki Nakatani,*[†] *Sreelakshmi K. S.,*[†] *Kohki Sasaki, Mika Nozaki, Ayumu Kondo, Tokuhisa Kawawaki, Saikat Das* and Yuichi Negishi**

Institute of Multidisciplinary Research for Advanced Materials, Tohoku University, Aoba-ku, Sendai 980-8577, Japan.

[†]These authors contributed equally.

*Correspondence to: das.saikat.c4@tohoku.ac.jp (S.D.), yuichi.negishi.a8@tohoku.ac.jp (Y.N.)

Table of Contents

Experimental details

Materials

All reagents and solvents were procured from commercial vendors and used as received without additional purification unless stated otherwise. Copper(II) nitrate trihydrate ($Cu(NO_3)_2 \cdot 3H_2O$), triethylamine (NEt_3), trifluoroacetic acid (CF_3COOH), and 1,4-dioxane were obtained from FUJIFILM Wako Pure Chemical Corporation. Acetonitrile (MeCN), dichloromethane (DCM), and dimethylacetamide (DMAc) were obtained from Kanto Chemical Co., Inc. *tert*-butyl mercaptan, and creatinine were obtained from Tokyo Chemical Industry Co., Ltd. But-2-yne-1,4-diyl diisonicotinate (bddi) and 2,5-Di(pyridin-4-yl)thiophene (dptp) were obtained from ET Co., Ltd. Pure Milli-Q water (>18 MΩ · cm) was generated using a Merck Millipore Direct 3 UV system.

Methods

Single-crystal X-ray diffraction (SCXRD): For SCXRD measurements, high-quality single crystals were immersed in cryoprotectant Parabar 10312 (Hampton Research, 34 Journey, Aliso Viejo, CA 92656-3317 USA) and mounted on Dual-Thickness MicroMounts™ (MiTeGen, LLC, Ithaca, NY, USA). Diffraction data for the single crystals were collected on a Bruker D8 QUEST and a XtaLAB Synergy-DW SCXRD diffractometers equipped with monochromatic Mo Kα radiation (λ = 0.71073 Å) and Cu Kα radiation (λ = 1.5418 Å), respectively. Crystal structures were solved using the Apex5 Bruker software suite[1] for measurements collected on the D8 QUEST, and CrysAlisPro[2] for the XtaLAB Synergy-DW datasets. The crystals used for diffraction of **Cu_{10}-dptp** were extremely small (≈ 0.010 × 0.015 × 0.075 mm) and mechanically fragile, frequently developing microcracks during manipulation and cryogenic cooling. As a result, the diffraction intensity was weak and data completeness at high resolution was limited. Attempts to collect data at elevated temperatures using newly selected crystals were unsuccessful due to rapid degradation of crystal quality and insufficient diffraction intensity. Consequently, the dataset presented here represents the best quality attainable for this material. During refinement, inappropriate global restraints were removed and replaced by localized, chemically justified restraints applied only to disordered regions (notably the trifluoroacetate and tert-butyl groups), resulting in physically reasonable displacement parameters and a stable model. Despite the moderate R values, the

structural model reliably establishes the decanuclear Cu_{10} cluster geometry and the connectivity of the extended framework.

Optical microscopy: Optical microscopy images were acquired on an Olympus SZX7 stereo microscope.

Powder X-ray diffraction (PXRD): PXRD data were obtained on a Rigaku MiniFlex X-ray diffractometer equipped with a CuKα radiation source (λ = 1.5418 Å), operated at 40 kV and 15 mA. Data were recorded over a 2θ range of 5º–35º, using a step size of 0.02º and a scan speed of 2.0º per min.

Nitrogen sorption: N_2 physisorption isotherms were recorded at 77 K on a Quantachrome Autosorb iQ3 gas sorption analyzer. Before data acquisition, samples were pretreated by degassing at 50 °C for 8 h employing a turbomolecular vacuum pump. The multipoint Brunauer–Emmett–Teller (BET) method was applied to the nitrogen uptake data to calculate the specific surface area.

X-ray photoelectron spectroscopy (XPS): XPS measurements were performed on a JPS-9-1-MC electron spectrometer (JEOL, Tokyo, Japan) using Mg K_α radiation (1253.6 eV) as the excitation source. Binding energies were calibrated against the neutral C 1s signal at 283.3 eV.

Scanning electron microscopy (SEM): SEM coupled with energy-dispersive X-ray spectroscopy (SEM-EDX) was conducted on a JEOL JSM-7800F field-emission scanning electron microscope equipped with an Oxford X-Max EDX detector.

Thermogravimetric analysis (TGA): TGA was carried out on a Thermo Plus EVO2 instrument by heating the sample from room temperature to 800 °C at a rate of 10 °C min^{-1} under a nitrogen flow of 50 mL min^{-1}.

UV-Vis absorption spectra: UV-Vis absorption spectra were measured on a JASCO V-770 spectrophotometer.

Photoluminescence (PL): PL spectra were acquired using an Edinburgh Instruments (EI) FLS1000 spectrofluorometer equipped with a continuous (450 W) xenon lamp.

Fourier-transform infrared (FT-IR): FT-IR spectra were collected using a JASCO FT/IR-4700 spectrometer operated in attenuated total reflectance (ATR) mode, covering the range of 4000–500 cm^{-1}.

Synthesis methods

Synthesis of $[CuS^tBu]_n$ complex

CuS^tBu was synthesized following a previously described protocol.[3] Briefly, a solution of copper(II) nitrate trihydrate (3.0 mmol) in acetonitrile (10.0 mL) was treated with triethylamine (10.0 mL), generating a blue precipitate. Subsequent addition of *tert*-butyl mercaptan (9.0 mmol) under continuous stirring dissolved the precipitate and afforded a yellow solution. After solvent evaporation, the solid residue was washed with methanol and dried, affording the yellow product in ~95% yield.

Synthesis of $[Cu_{10}(S^tBu)_6(CF_3COO)_4\ (bddi)_4]$ (Cu_{10}-bddi)

A suspension of the $[CuS^tBu]_n$ complex (0.065 mmol) was prepared in 1 mL of DCM. To this mixture, CF_3COOH (0.09 mmol) was added under continuous stirring at room temperature until a clear solution was obtained. Subsequently, a freshly prepared solution of the bddi linker (0.065 mmol in 1 mL of 1,4-dioxane) was introduced dropwise. The reaction mixture was left undisturbed at ambient temperature for three days, allowing slow crystallization to occur. Block-shaped orange crystals formed at the interface between the immiscible phases, giving an isolated yield of 18.33% (based on Cu).

Synthesis of $[Cu_{10}(S^tBu)_6(CF_3COO)_4\ (dptp)_4]$ (Cu_{10}-dptp)

A suspension of the $[CuS^tBu]_n$ complex (0.065 mmol) was prepared in 1 mL of DCM. To this mixture, CF_3COOH (0.09 mmol) was added under continuous stirring at room temperature until a clear solution was obtained. Subsequently, a freshly prepared solution of the dptp linker (0.065 mmol in 1 mL of DMAc) was introduced dropwise. The reaction mixture was left undisturbed at ambient temperature for two days, allowing slow crystallization to occur. Enongated prismatic yellow crystals formed at the interface between the immiscible phases, giving an isolated yield of 14.22% (based on Cu).

Sensing of creatinine using Cu_{10}-bddi and Cu_{10}-dptp

For fluorescence-based creatinine detection, approximately 1 mg of the **Cu_{10}-bddi** or **Cu_{10}-dptp** material was finely ground and subsequently dispersed in 3 mL of deionized water by brief ultrasonication. The use of pure water (i.e., without any buffer) ensured that the intrinsic microenvironment of the clusters remained unaltered and that no extraneous ions interfered with the sensing response. After obtaining a uniform colloidal dispersion, aqueous creatinine solutions of varying concentrations were incrementally added to the suspension to initiate the sensing process. The resulting mixtures were transferred into a standard quartz cuvette for luminescence measurements. Photoluminescence spectra were acquired using a fluorescence spectrophotometer, and the excitation wavelength was selected based on the intrinsic absorption characteristics of each material: λ_{ex} = 275 nm for **Cu_{10}-bddi**, λ_{ex} = 355 nm for **Cu_{10}-dptp**. Fluorescence responses were quantified by monitoring the intensity changes at the characteristic emission maxima: 301 nm for **Cu_{10}-bddi**, 391 nm for **Cu_{10}-dptp**. All measurements were conducted at ambient temperature, and each concentration-dependent experiment was repeated three times to ensure statistical validity and reproducibility of the sensing performance.

Recycling test

To evaluate the reusability of the sensing material, the solid **Cu_{10}-bddi** or **Cu_{10}-dptp** sample was recovered after each sensing cycle by centrifugation. The collected solids were thoroughly washed multiple times with deionized water to remove residual creatinine and any loosely adsorbed species. After washing, the material was re-dispersed in fresh deionized water, and the fluorescence-based creatinine detection experiment was repeated following the same procedure as the initial cycle.

Table S1. Crystal data and structure refinement parameters of **Cu_{10}-bddi**

Identification code	Cu_{10}-bddi
Empirical formula	$C_{32.75}H_{40.50}Cl_{1.50}Cu_5F_6N_2O_8S_3$
CCDC number	2503061
Formula weight	1171.22
Temperature/K	90
Crystal system	Triclinic
Space group	*P*-1
a/Å	11.8657(4)
b/Å	13.8123(5)
c/Å	16.9216(6)
α/°	96.7110(10)
β/°	103.7890(10)
γ/°	105.7790(10)
Volume/Å^3	2542.46(16)
Z	2
ρ_{calc}/g cm^{-3}	1.530
μ/mm^{-1}	2.322
F(000)	1175
Radiation	MoKα (λ = 0.71073 Å)
2Θ range for data collection/°	2.527 to 27.515°
Index ranges	-15<=h<=15, -17<=k<=17, -21<=l<=21
Reflections collected	30950
Independent reflections	10998 [R_{int} = 0.0329]
Data/restraints/parameters	10998/62/542
Goodness-of-fit on F^2	1.055
Final R indexes [I>=2σ (I)]	R1 = 0.0520, wR2 = 0.1675
Final R indexes [all data]	R1 = 0.0552, wR2 = 0.1707
Largest diff. peak/hole / e Å^{-3}	1.94/-0.36

Table S2. Crystal data and structure refinement parameters of **Cu_{10}-dptp**

Identification code	Cu_{10}-dptp
Empirical formula	$C_{30.52}H_{38.17}Cu_5F_6N_{2.13}O_{4.13}S_4$
CCDC number	2503062
Formula weight	1060.88
Temperature/K	90
Crystal system	Monoclinic
Space group	$P2_1/c$
a/Å	14.1620(5)
b/Å	12.3712(6)
c/Å	23.7398(9)
α/°	90
β/°	99.157(4)
γ/°	90
Volume/Å^3	4106.2(3)
Z	4
ρ_{calc}/g cm^{-3}	1.716
μ/mm^{-1}	5.320
F(000)	2129
Radiation	CuKα (λ = 1.54184 Å)
2Θ range for data collection/°	3.161 to 65.088°
Index ranges	-16<=h<=16, -4<=k<=14, -27<=l<=27
Reflections collected	17028
Independent reflections	6907 [R_{int} = 0.0511]
Data/restraints/parameters	6907/90/445
Goodness-of-fit on F^2	0.944
Final R indexes [I>=2σ (I)]	R1 = 0.0955, wR2 = 0.1736
Final R indexes [all data]	R1 = 0.1810, wR2 = 0.2199
Largest diff. peak/hole / e Å^{-3}	1.100/-1.429

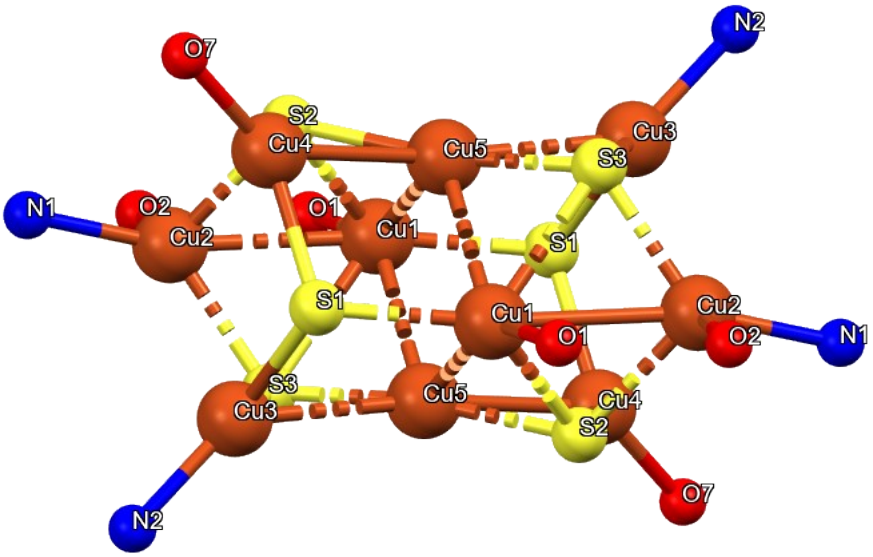

Fig. S1 Annotated structural illustration of the Cu_{10} nanocluster stabilized by six tert-butylthiolate and four trifluoroacetate ligands, further coordinated by four bddi linkers in **Cu_{10}-bddi**.

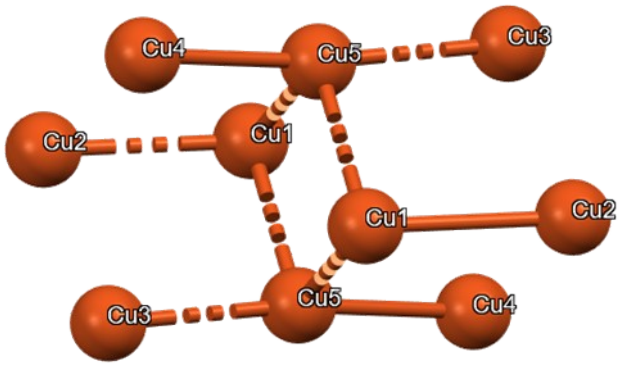

Fig. S2 Annotated representation of the Cu_{10} core.

Table S3. Detailed Cu–Cu bond length data for the Cu_{10} core represented in Fig. S2

Atom1	Atom2	Bond length / Å		Bond length / Å
Cu1	Cu2	2.747	Maximum	2.838
Cu1	Cu5	2.838	Minimum	2.651
Cu1	Cu5	2.710	Average	2.744
Cu3	Cu5	2.775	S.D.	0.063
Cu4	Cu5	2.651		

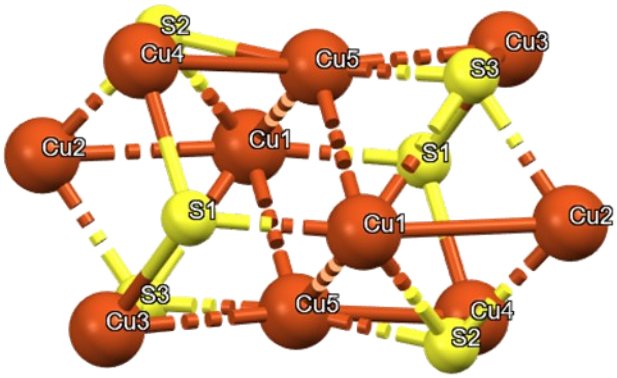

Fig. S3 Arrangement of six thiolate ligands attached to the Cu_{10} core.

Table S4. Summary of Cu–S bond lengths corresponding to the ligand arrangement in Fig. S3

Atom1	Atom2	Bond length / Å		Bond length / Å
Cu1	S1	2.264	Maximum	2.598
Cu1	S2	2.421	Minimum	2.171
Cu1	S3	2.598	Average	2.290
Cu2	S2	2.341	S.D.	0.118
Cu2	S3	2.275		
Cu3	S1	2.219		
Cu3	S3	2.259		
Cu4	S1	2.215		
Cu4	S2	2.244		
Cu5	S2	2.186		
Cu5	S3	2.171		

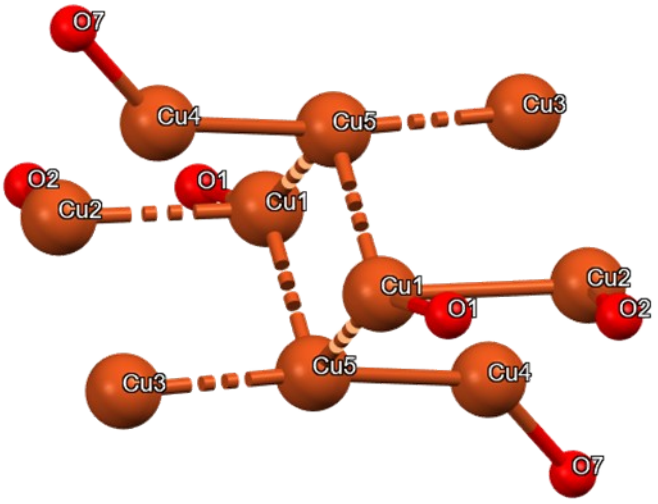

Fig. S4 Attachment pattern of four trifluoroacetate ligands to the Cu_{10} cluster.

Table S5. Summary of Cu–O bond lengths corresponding to the ligand arrangement in Fig. S4

Atom1	Atom2	Bond length / Å		Bond length / Å
Cu1	O1	2.072	Maximum	2.128
Cu2	O2	2.128	Minimum	1.981
Cu4	O7	1.981	Average	2.060
			S.D.	0.061

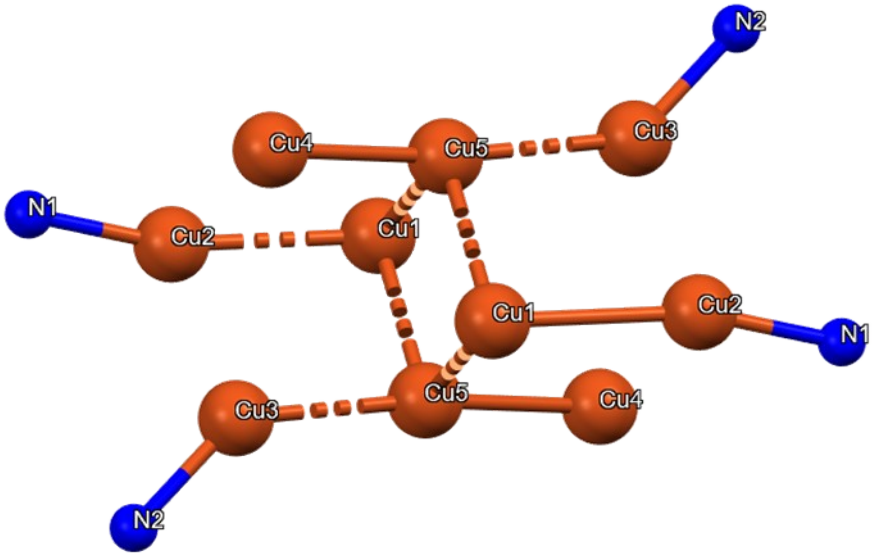

Fig. S5 Attachment pattern of four linker molecules to the Cu_{10} cluster.

Table S6. Summary of Cu–N bond lengths referring to Fig. S5

Atom1	Atom2	Bond length / Å		Bond length / Å
Cu2	N1	2.013	Maximum	2.013
Cu3	N2	1.989	Minimum	1.989
			Average	2.001
			S.D.	0.012

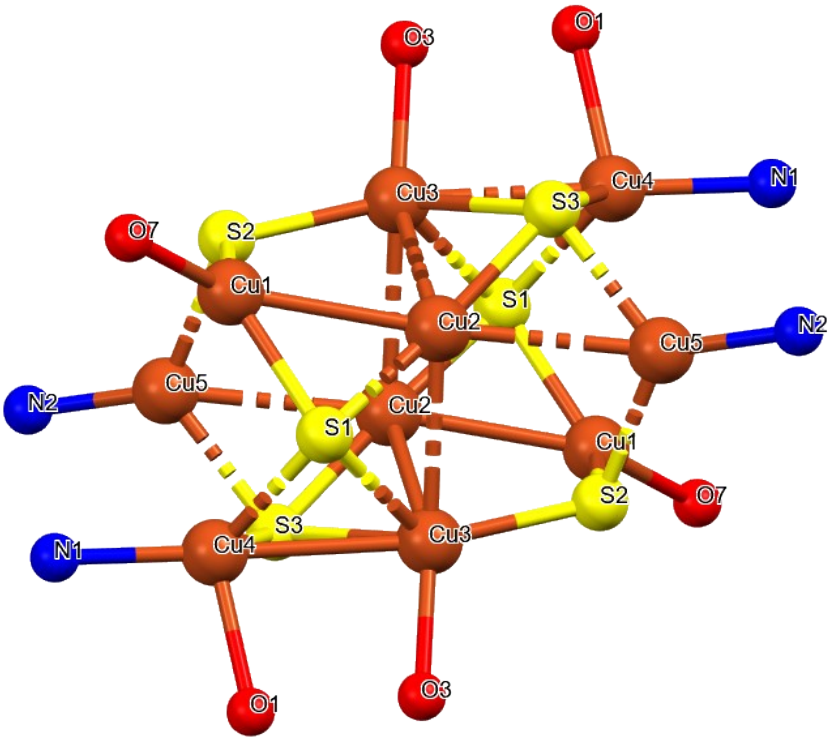

Fig. S6 Annotated structural illustration of the Cu_{10} nanocluster stabilized by six tert-butylthiolate and four trifluoroacetate ligands, further coordinated by four dptp linkers in **Cu_{10}-dptp**.

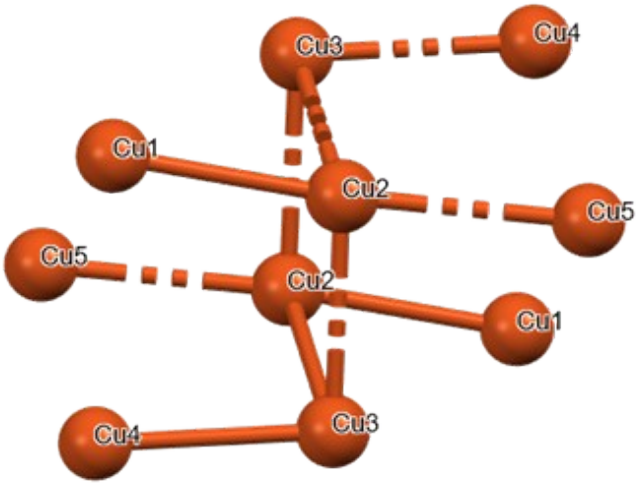

Fig. S7 Annotated representation of the Cu_{10} core.

Table S7. Detailed Cu–Cu bond length data for the Cu_{10} core represented in Fig. S7

Atom1	Atom2	Bond length / Å		Bond length / Å
Cu1	Cu2	2.657	Maximum	2.838
Cu2	Cu3	2.730	Minimum	2.657
Cu2	Cu3	2.838	Average	2.755
Cu2	Cu5	2.814	S.D.	0.065
Cu3	Cu4	2.734		

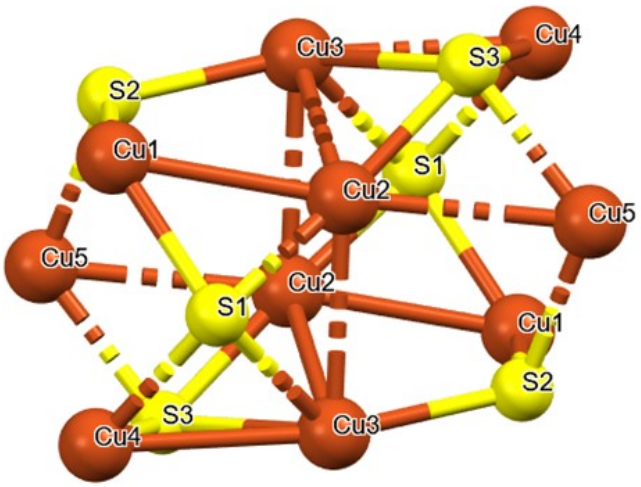

Fig. S8 Arrangement of six thiolate ligands attached to the Cu_{10} core.

Table S8. Summary of Cu–S bond lengths corresponding to the ligand arrangement in Fig. S8

Atom1	Atom2	Bond length / Å		Bond length / Å
Cu1	S1	2.210	Maximum	2.560
Cu1	S2	2.218	Minimum	2.150
Cu2	S1	2.165	Average	2.279
Cu2	S3	2.150	S.D.	0.117
Cu3	S1	2.445		
Cu3	S2	2.250		
Cu3	S3	2.560		
Cu4	S1	2.277		
Cu4	S3	2.319		
Cu5	S2	2.221		
Cu5	S3	2.252		

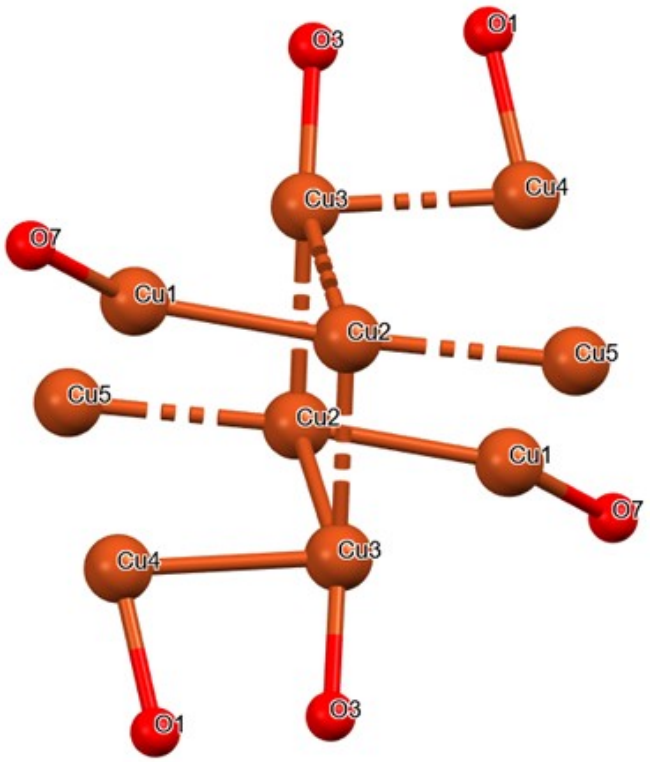

Fig. S9 Attachment pattern of four trifluoroacetate ligands to the Cu_{10} cluster.

Table S9. Summary of Cu–O bond lengths corresponding to the ligand arrangement in Fig. S9

Atom1	Atom2	Bond length / Å		Bond length / Å
Cu1	O7	2.020	Maximum	2.100
Cu3	O3	2.043	Minimum	2.020
Cu4	O1	2.100	Average	2.054
			S.D.	0.034

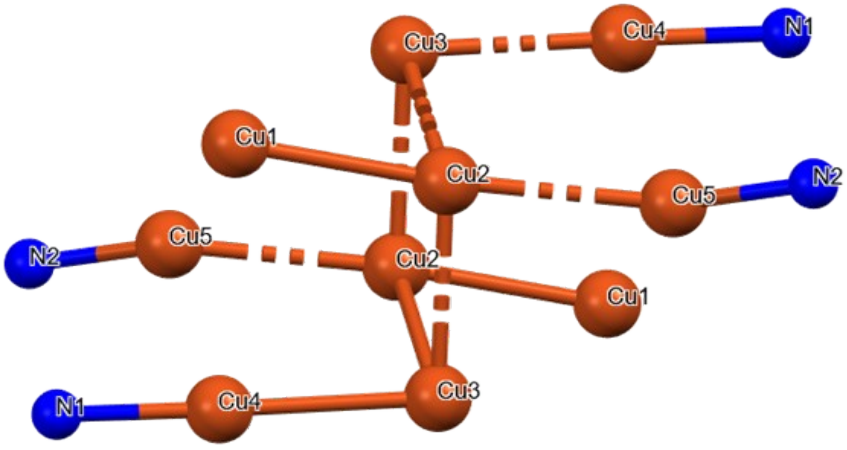

Fig. S10 Attachment pattern of four linker molecules to the Cu_{10} cluster.

Table S10. Summary of Cu–N bond lengths referring to Fig. S10

Atom1	Atom2	Bond length / Å		Bond length / Å
Cu4	N1	2.020	Maximum	2.020
Cu5	N2	1.970	Minimum	1.970
			Average	1.995
			S.D.	0.025

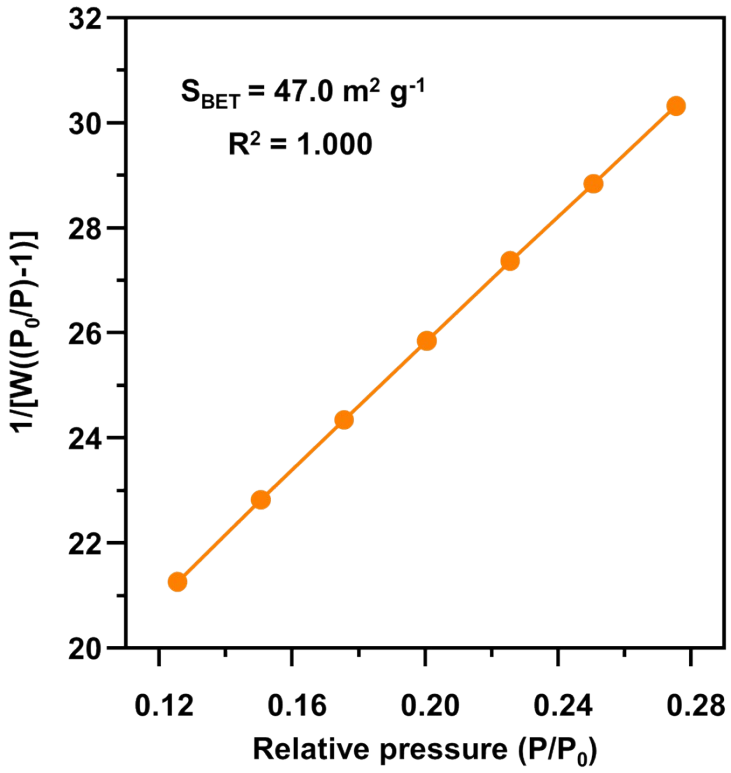

Fig. S11 BET plot for **Cu_{10}-bddi** calculated from the N_2 adsorption isotherms at 77 K.

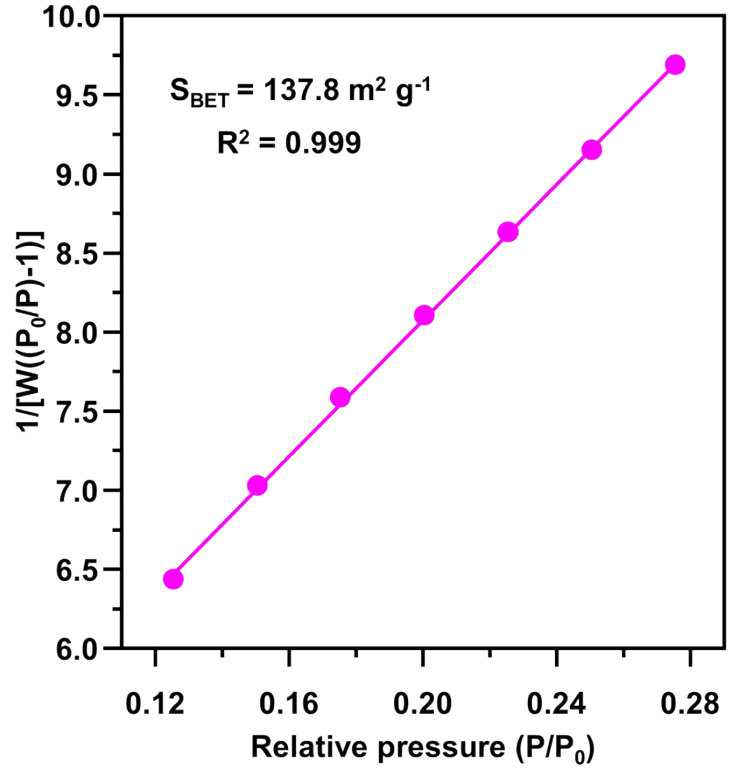

Fig. S12 BET plot for **Cu_{10}-dptp** calculated from the N_2 adsorption isotherms at 77 K.

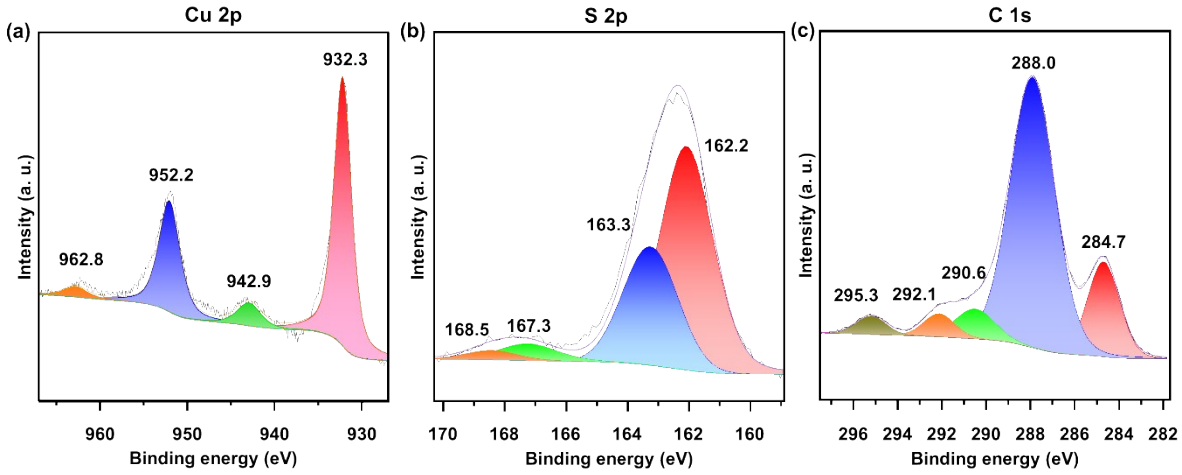

Fig. S13 High-resolution XPS spectra of (a) Cu 2p, (b) S 2p, and (c) C 1s regions for **Cu_{10}-bddi**.

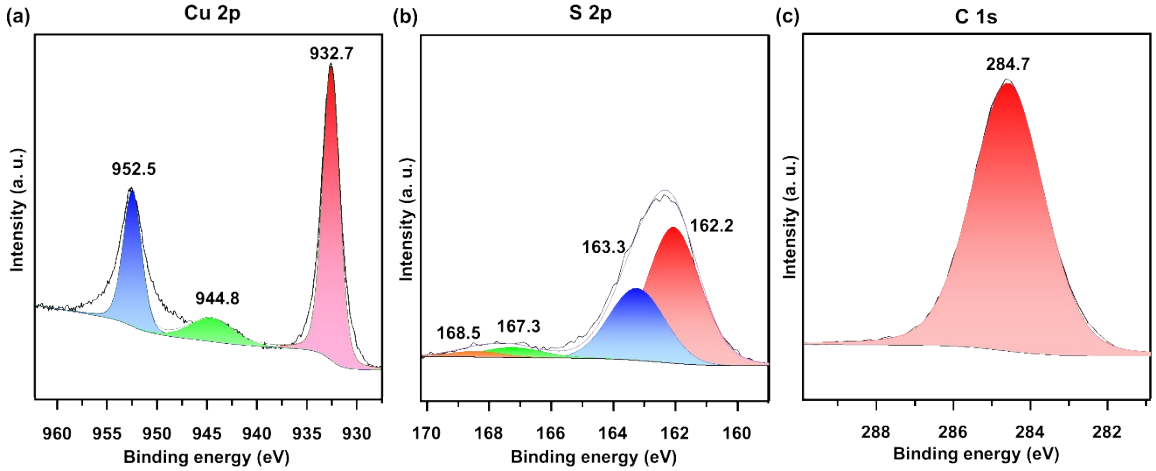

Fig. S14 High-resolution XPS spectra of (a) Cu 2p, (b) S 2p, and (c) C 1s regions for **Cu_{10}-dptp**.

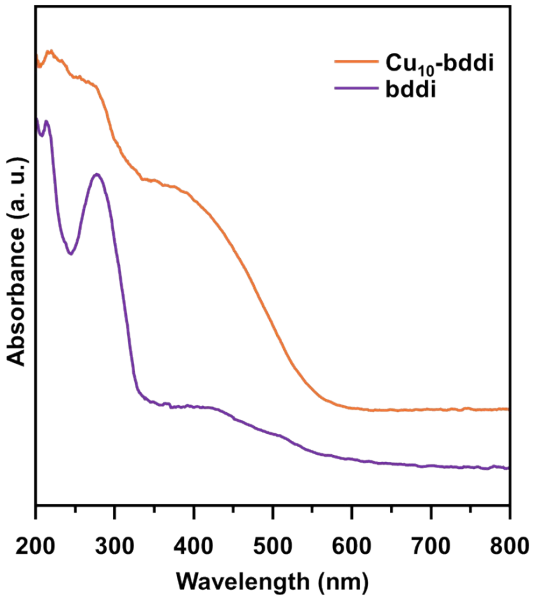

Fig. S15 Solid-state UV-Vis absorbance spectra of **Cu_{10}-bddi** and bddi linker.

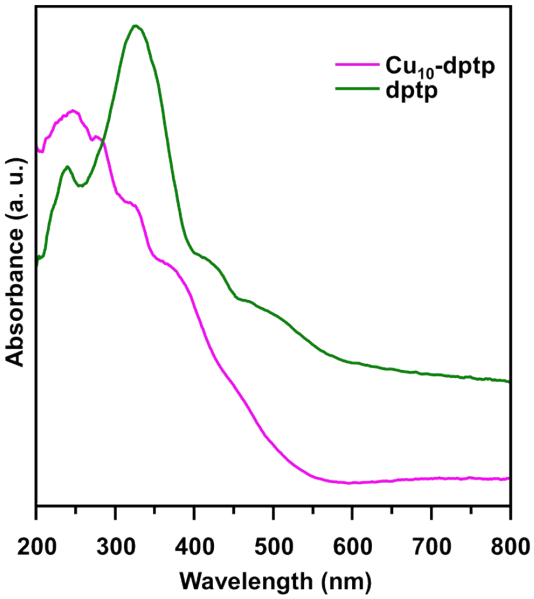

Fig. S16 Solid-state UV-Vis absorbance spectra of **Cu_{10}-dptp** and dptp linker.

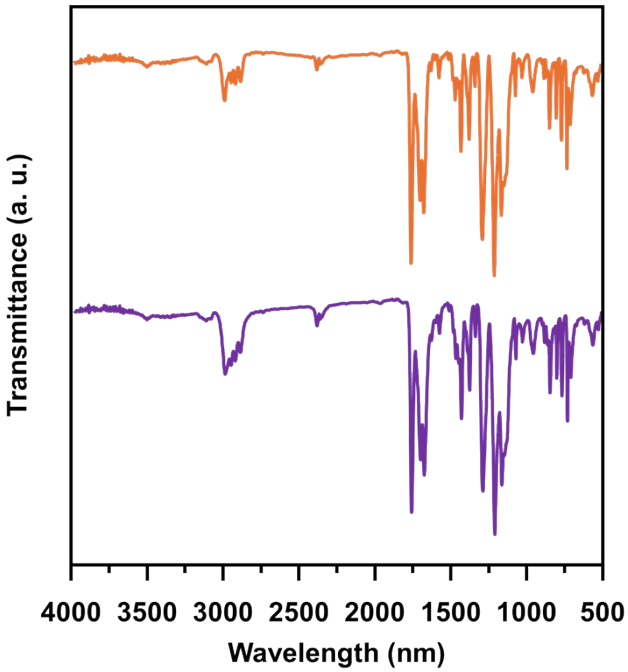

Fig. S17 FT-IR spectra of pristine **Cu_{10}-bddi** (orange) and after sensing creatinine (purple). The multiple absorptions observed between ~3050 and ~2850 cm^{-1} correspond to C–H stretching modes of the tert-butylthiolate and pyridyl ligands. A strong band at ~1650 cm^{-1}, present in both spectra, is assigned to the asymmetric carboxylate stretching vibration $\nu_{as}(COO^-)$ of the coordinated CF_3COO^- groups, while the corresponding symmetric stretch $\nu_s(COO^-)$ appears as intense features between ~1380–1320 cm^{-1}. Signals in the ~1600–1500 cm^{-1} region arise from in-plane ring deformations and C=C/C=N stretching modes of the coordinated pyridyl units. The prominent and complex absorptions spanning ~1250–1100 cm^{-1} are attributed to C–F stretching and C–O vibrations of the CF_3COO^- ligands. Out-of-plane C–H deformation modes of the pyridyl rings appear between ~900–800 cm^{-1}, whereas the bands in the ~780–700 cm^{-1} region are consistent with C–S stretching vibrations of the tert-butylthiolate groups. Weak absorptions below ~650 cm^{-1} are assigned to Cu–S, Cu–O, and Cu–N coordination vibrations associated with the Cu_{10} cluster core.

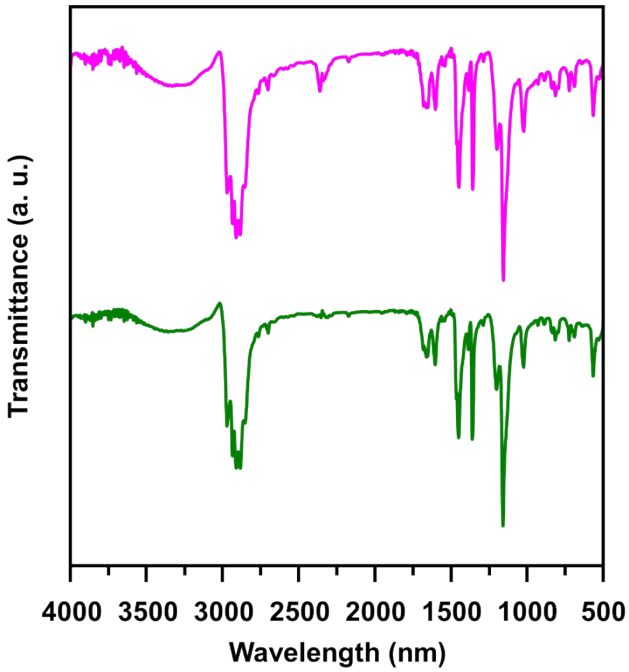

Fig. S18 FT-IR spectra of pristine **Cu_{10}-dptp** (pink) and after sensing creatinine (green). Both spectra exhibit multiple absorptions in the 3050–2850 cm^{-1} range, corresponding to ν(C–H) stretching vibrations of the tert-butylthiolate ligands, along with weaker aromatic ν(C–H) stretches above 3000 cm^{-1}. A strong band observed at ca. 1690–1670 cm^{-1} is assigned to the ν(C═O) stretching mode of the coordinated CF_3COO^- anions. The features at ca. 1610–1580 cm^{-1} arise from ring ν(C═C)/ν(C═N) stretching vibrations of the pyridyl linkers. Multiple bands appearing between 1470–1370 cm^{-1} correspond to δ(C–H) bending modes associated with both the tert-butyl and aromatic groups. Intense absorptions in the 1250–1150 cm^{-1} region, together with additional features between 1120–1000 cm^{-1}, are attributed to ν(C–F) and ν(C–O)/ν(C–N) vibrations originating from the CF_3COO^- anions and pyridyl moieties. Bands located between ~850 and 700 cm^{-1} correspond to out-of-plane C–H deformation modes of the pyridine and aryl rings as well as deformation vibrations of the CF_3COO^- groups. Weak absorptions below 650 cm^{-1} are assigned to Cu–S, Cu–N, and Cu–O coordination vibrations within the Cu_{10} cluster framework.

References

1. Bruker APEX5, v2019.1–0, Bruker AXS Inc., Madison, WI, USA, 2019.
2. Rigaku Oxford Diffraction, CrysAlisPro software system, version 1.171.40.54. Rigaku Corporation, Oxford, 2019.
3. S. Das, J. Sakai, R. Nakatani, A. Kondo, R. Tomioka, S. Das, S. Takahashi, S. Biswas and Y. Negishi, *Chem. Sci.*, 2025, 16, 2600-2608.